Catena 172 (2019) 255–265

Contents lists available at ScienceDirect

Catena

journal homepage: www.elsevier.com/locate/catena

Channel adjustment after artificial neck cutoffs in a meandering river of the Zoige basin within the Qinghai-Tibet Plateau, China

Zhiwei Li[a,b], Peng Gao[c,*]

[a] School of Hydraulic Engineering, Changsha University of Science & Technology, Changsha 410114, China
[b] State Key Laboratory of Plateau Ecology and Agriculture, Qinghai University, Xining 810016, China
[c] Department of Geography, Maxwell School of Citizenship and Public Affairs, College of Arts & Sciences, Syracuse University, Syracuse, NY 13244, USA

ARTICLE INFO

Keywords:
Meandering river
Neck cutoff
Channel adjustment
Diversion angle
Cantilever bank failure

ABSTRACT

Neck cutoff is an essential process that significantly changes the morphodynamic characteristics of a meandering bend. In reality, however, observing natural processes of a neck cutoff is very difficult. In this study, we artificially triggered neck cutoffs by excavating a 0.4 m (width) × 0.5 m (depth) ditch to connect the beginning and ending of two highly convoluted bends along a meandering tributary of the upper Black River, a major tributary of the Upper Yellow River situated in the northeastern side of the Qinghai-Tibet Plateau in China. Our morphologic and hydraulic measurements in summers of 2013, 2014, 2016, and 2017, the subsequent hydraulic-geometry analysis, and three-dimensional simulation showed that both artificial ditches expanded fast to the size comparable to the former channel in a three-year period and the oxbow channel was disconnected from the former channel quickly, though sediment supply may be limited in this area. The morphological adjustment was featured by (1) distinct temporal trends of the development of the width/depth ratio between the two cutoff channels, (2) different diversion factors of the total discharge to the cutoff channel, and (3) diverse interaction patterns between cutoff and former channels. These discrepancies were supported by simulated different three-dimensional velocity distributions in the two cutoff channels, suggesting the importance of the clustered local velocities. Comparing these results with those reported in earlier studies showed that besides channel slope, unit stream power, and bank strength, the diversion angle between the cutoff and former channel played an important role in controlling channel adjustment. The discrepancy of the adjustment processes between the cutoff channel in this study and those in two previous ones revealed that channel adjustment after neck cutoff behaved differently under different physical settings and require more field-based studies.

1. Introduction

Cutoff is a physical process influencing the evolution of a meandering channel in terrestrial and submarine environments (Guneralp et al., 2012; Hooke, 1984). Geometrically, cutoff reduces morphological complexity of meandering rivers regardless whether they evolve in old floodplains, subtropical grasslands, alpine meadows, tropical rainforests, permafrosts, desert edges, bedrock, submarine, or even Mars (Constantine et al., 2014; Deptuck et al., 2007; Finnegan and Dietrich, 2011; Li et al., 2017; Lonsdale and Hollister, 1979; Matsubara et al., 2015; Wasklewicz et al., 2004). Hydrodynamically, cutoff indicates in a short term that an intrinsic threshold of a meandering bend is reached (Knighton, 1998; Schumm, 1977) and maintains in the long-term the periodic migration of a meandering river by making their planform geometries simpler (Camporeale et al., 2007; Guneralp and Rhoads, 2009; Hooke, 2004; Seminara et al., 2001). As such, efforts of attempting to understand occurrence of cutoff and its temporal impacts on hydrodynamic processes of the associated meandering rivers have been made by establishing theoretical models, performing numerical simulation and laboratory experiments, and deploying field measurements (Camporeale et al., 2005; Erskine et al., 1992; Fisk, 1944; Frascati and Lanzoni, 2010; Friedkin, 1945; Gay et al., 1998; Hager, 2003; Hooke, 1995b; Ikeda et al., 1981; Luchi et al., 2011; Pang, 1986; Stolum, 1996; Stolum, 1998).

It is well known that many common modes of river planform evolution result in increased channel sinuosity, decreased bend curvature, and increased entrance angles of bends (Constantine et al., 2010a; Fisk, 1947; Hickin and Nanson, 1984; Hooke, 1995a; Hooke and Redmond, 1992; Howard and Knutson, 1984; Ikeda et al., 1981). Their consequence is channel cutoff. Yet, mechanics of cutoff and the succeeding

* Corresponding author.
E-mail address: pegao@maxwell.syr.edu (P. Gao).

https://doi.org/10.1016/j.catena.2018.08.042
Received 1 February 2018; Received in revised form 28 August 2018; Accepted 31 August 2018

channel adjustment still have not been fully understood due to the complexity of cutoff processes, which is primarily reflected in three aspects. First, different sets of hydrodynamic mechanisms dominate effects of individual cutoffs on meandering channels over short-time periods and those of intermittent cutoffs on multiple loops of meandering reaches (Camporeale et al., 2008; Frascati and Lanzoni, 2009). Second, long-term (at least decades) meandering dynamics and its interaction with cutoff processes for small meandering rivers with widths < 10 m are hard to explore due to scarcity of high-resolution imagery data (Hooke, 2004). The commonly available historical maps and aerial photographs with coarse resolutions merely entail extracting geometric parameters of meanders and bends for large meandering rivers with wide channel widths (mostly no less than 40 m) and subsequently using them to develop statistical or process-based relationships (Constantine and Dunne, 2008; Erskine, 1992; Gutierrez and Abad, 2014; Hudson and Kesel, 2000; Micheli and Larsen, 2011; Morais et al., 2016; Nicoll and Hickin, 2010; Ollero, 2010; Wellmeyer et al., 2005). Third, different processes cause two fundamentally different types of cutoff, chute and neck cutoff (Hooke, 1984). The former is primarily caused by continuous enlargement of swales, propagation of headcut on the concave bank, or relatively large flows in flood seasons eroding through the inner bank or point bars of the bend, while the latter results from the self-intersection between downstream and upstream bends of a meandering river via overbank flow erosion or progressive bank failure (Constantine et al., 2010b; Erskine et al., 1992; Gay et al., 1998; Guneralp and Marston, 2012; Li et al., 2017). The morphological distinction between chute and neck cutoff is equally significant. A neck cutoff may happen when the shortest distance between the two bend limbs is about one channel width (Howard, 1992; Howard and Knutson, 1984; Ikeda et al., 1981; Stolum, 1996), whereas a chute cutoff may take place when this distance is > 10 channel width (Stolum, 1998).

Chute cutoff short-circulates a meandering channel (Stolum, 1998). Its frequency of occurrence is generally higher than that of neck cutoff (Lewis and Lewin, 1983; Micheli and Larsen, 2011), which may explain the increased number of field-based studies on chute cutoffs in the context of meandering processes (Fuller et al., 2003; Gay et al., 1998; Ghinassi, 2011; Hauer and Habersack, 2009; Le Coz et al., 2010; Thompson, 2003; Zinger et al., 2011). Also noticeable is that chute cutoff tends to be much easier reproduced in flume experiments than its counterpart (Braudrick et al., 2009; Howard, 2009; Peakall et al., 2007; van Dijk et al., 2012). Many studies have identified some control factors such as height of floodplain, sediment supply, discharge regime, and channel bifurcation (Aslan et al., 2005; Camporeale et al., 2008; Grenfell et al., 2012; Zinger et al., 2011) that may lead to a chute cutoff. Nonetheless, debates on mechanisms of chute cutoff still continues (Hooke, 2013).

Neck cutoff is typically a result of meandering channel evolution for a long time period and hence serves as an end point of a meander evolution cycle (Hooke, 2013). Early studies have indicated that neck cutoff tends to occur in narrow channels with well-vegetated banks and low channel gradients (Brice, 1984; Howard and Knutson, 1984; Nanson and Hickin, 1983). Neck cutoff may also be triggered by accelerated bank erosion due to the weakened bank strength cause by seepage flow (Han and Endreny, 2014). However, very few studies have focused on channel adjustment following the occurrence of neck cutoff. Two reported studies using field-measured data were based on natural neck cutoffs in two different types of rivers (Hooke, 1995b; Hooke, 2004; Konsoer and Richards, 2016). The first was in reaches of Bollin and Dane rivers in northwest England with the mean channel width and depth of approximately 8 and 1 m, respectively (Hooke, 1995b; Hooke, 2004). The second was in the lower White River in Arkansas, USA, whose mean channel width was 170 m and mean channel depth was 7 m (Konsoer and Richards, 2016). Their width-depth ratios are different in more than one order of magnitude, suggesting that neck cutoffs may occur in meandering channels with diverse sizes. Whether the same set of hydrodynamic processes controls both the occurrence of neck cutoffs and the subsequent channel adjustment requires more field-based measurements relevant to neck cutoffs to support and/or validate mechanics characterized by many hydrodynamic models (Guneralp and Marston, 2012; Hooke, 2013).

Unfortunately, cutoff typically happens in days or weeks (Eekhout and Hoitink, 2015; Hooke, 1995a; Pan et al., 1978; Zinger et al., 2011). Comparing with the prolonged evolution time of meanders, the cutoff period is very short. Thus, it is extremely difficult to capture the cutoff process in practice. Particularly, for meanders in the remote region located in the Qinghai-Tibet plateau of western China, the Zoige basin, even measuring channel morphology is pragmatically challenging. This might be why almost nothing is known about meandering dynamics and cutoff processes in these alpine rivers thus far. To fill this gap, we manually created cutoffs in a small meander tributary within the Zoige basin and measured the subsequent morphological adjustment of the channel, as well as the associated hydraulic variables. Different from the generation of classic artificial cutoffs that typically aimed at achieving certain engineering goals of flood control and inland river navigation (Bray and Cullen, 1976; Erskine, 1992; Pan et al., 1978; Smith and Winkley, 1996), our purpose was to provide the first-hand data describing the morphological adjustment of meanders after a cutoff in this area.

In this study, we reported our findings based on morphological and hydraulic data obtained in situ in Julys of 2013, 2014, 2016, and 2017 after excavating two ditches across the necks of two highly sinuous bends in the Zoige basin in 2013. By analyzing changes of typical cross sections in the cutoff and original/former channels and establishing their hydraulic geometry, we characterized the adjustment patterns of these different channels immediately after neck cutoff. Then, we performed three-dimensional flow simulation using MIKE 3 Flow Model to demonstrate spatial distributions of flow velocity within these channels and linked these spatially variable hydraulic parameters to the morphological changes of the channels. At last, we identified factors controlling evolution of these channels and compared our results with those in other regions.

2. Materials and methodology

2.1. Study sites and artificial neck cutoffs

The Zoige basin is located on the northeastern side of the Qinghai-Tibet Plateau in China (Fig. 1a) with elevations varying between 3400 and 3900 m (Nicoll et al., 2013). It is surrounded by high mountains formed by orographic movement about 14 million years ago and covered by relatively smooth topography, which was derived from the quick filling of lacustrine and fluvial sediment roughly 900 kyr ago (Wang et al., 1995). On top of the filled sediment were the unique alpine peats (mostly 1–3 m thick) and the grasslands degraded from these peats (Xiao et al., 2010). Two main rivers within the basin are White and Black Rivers, running in the southeast-northwest direction and finally joining the Upper Yellow River in the plateau (Fig. 1b). The Black River, originating from the western Min Mountain, is 456 km long with a drainage area of 7600 km^2 and an average channel gradient of 0.00016. Its annual average discharge and sediment concentration are 32.6 m^3/s and 0.33 kg/m^3, respectively. Maiqu River is the mainstream of the upper Black River with the maximum channel width of around 30 m (Fig. 1b). Neck cutoffs have left hundreds of oxbow lakes and abandoned channels over a long time period along this river. A second-order tributary situated in a small upland in the upstream of the Maiqu River was selected for this study (Fig. 1b). Its channel is highly sinuous and dominated by bends of variable sizes with less elongated Ω shapes. Neck cutoffs and the resultant oxbow lakes are discernible along the study reach. Although rivers possessing similar planforms with highly convoluted loops and cutoffs have been reported elsewhere (Ebisemiju, 1993; Gautier et al., 2007; Gilvear et al., 2000), the dominance of the

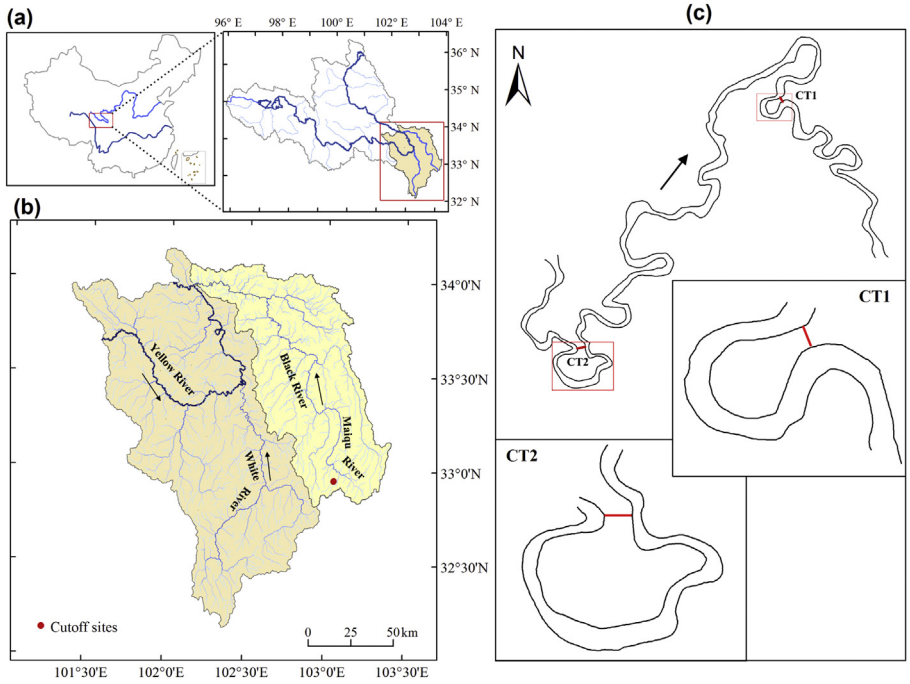

Fig. 1. Geographic location of the study area and sites. (a) location of the study area; (b) pattern of the stream network in the study area; (c) geometries of the two bends subject to artificial neck cutoff (CT1 and CT2).

alpine climate and the existence of peatland mark the unique physical settings of the study river reach.

Two highly convoluted meander bends (CT1 and CT2) within the reach (Fig. 1c) were selected for generating artificial cutoffs because these sites are not far (about 1200 m) from the road and the neck widths between the upstream and downstream limbs are relatively short, 2.2 m in CT1 (32° 56′ 55.5″ N, 103° 03′ 12.9″ E) and 5.9 m in CT2 (32° 56′ 47.4″ N, 103° 03′ 06.3″ E) (Fig. 1c). The meandering section from CT2 to the junction with the mainstream of the Maiqu River is about 6663 m long and has a sinuosity of 2.2 with the mean channel gradient of 0.0036. The channel distance between CT1 and CT2 (CT1 is downstream of CT2) is roughly 680 m (Fig. 1c). The catchment at the CT1 has an area of 31.7 km^2 without any gauged station and is mainly covered by thin peats and dense alpine meadow. Banks along the two bends have a composite vertical profile that may be divided into three layers from top to the bottom, the root-soil mixture, the silt and clay, and the gravel and sand (Fig. 2).

Despite similar shapes, CT1 and CT2 have distinct morphological characteristics. The mean channel width is 4.1 m for CT1 with that of 4.2 m at the apex and 3.5 m for CT2 with that of 6.5 m at the apex (Table 1). The bend curved length of CT1 and CT2 is 53 m and 130 m, respectively. At CT1, the radius of curvature at the apex point is 7.5 m, while at CT2, it is 16 m, which lead to their bend curvature (i.e., the ratio of radius of curvature to average channel width) of 1.8 and 4.6, respectively (Table 1). We manually excavated a ditch at the narrowest location of two bends with a rectangular cross section of about 0.4 m wide, and 0.5 m deep, on July 5 and 6, 2013, respectively (Fig. 3). This gave rise to a similar cutoff ratio, which is defined as the ratio of the path length of a bend to the length of the chord across the same two points (Hooke, 1995a; Hooke, 1995b), for CT1 and CT2 (Table 1). Practically, the size of the ditch was determined by the capacity of manpower on the site. Theoretically, this size is not critical for investigating channel adjustment after cutoff. Essentially, cutoff is a perturbation of meander evolution, which arguably is a non-equilibrium, continuous process (Hooke, 2013). A cutoff with any magnitude (i.e., the size of the ditch) will finally entail the former meander channel to become either a self-organized criticality (Hooke, 2004; Stolum, 1996; Stolum, 1998) or a more complex status (Frascati and Lanzoni, 2010; Perucca et al., 2005). Furthermore, this study focused more on the potential difference of channel adjustment between CT1 and CT2 under a similar disturbance (i.e., the similar size of the ditch). Therefore, the size of the excavated ditch is sufficient for the purpose of this study. To clarify the terminology, we denote the channel section including the meander bend before ditch excavation and its immediate upstream and downstream portions as the former/original channel, the excavated ditch and its subsequently evolved channel as the cutoff channel, and the meander bend separated by the cutoff channel as the abandoned or oxbow channel, respectively.

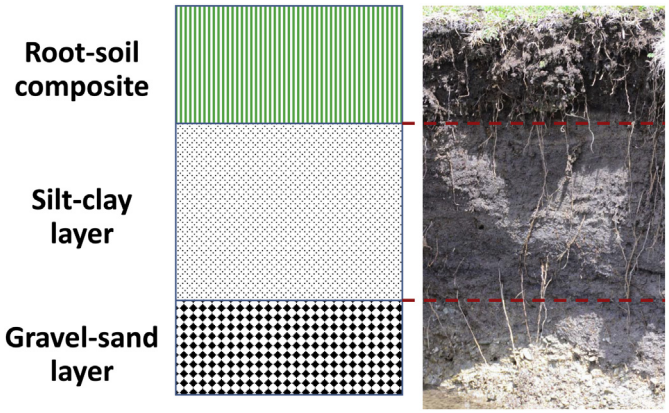

Fig. 2. Composition of materials along a vertical profile of a typical meandering bank in the study area.

2.2. Field methods

Representative cross sections of the cutoff and former channels were surveyed and the associated hydraulic variables were measured in the summer of 2013, 2014, and 2016, respectively. The day after ditch excavation in July of 2013, channel cross section profiles at three different locations of the cutoff channel in CT1 and CT2 were surveyed using a theodolite. At each cross section, mean flow width and depth

Table 1
Morphological features of CT1 and CT2.

Location	Bend curved length (m)	Neck width (m)	Channel width at apex (m)	Channel width (m)	Neck width (m)	Radius of curvature (m)	Bend curvature	Cutoff ratio
CT1	53	2.2	4.2	4.1	2.2	7.5	1.8	25.0
CT2	130	5.9	6.5	3.5	5.9	16.0	4.6	24.6

were measured using a staff gauge, while mean flow velocity was measured using a velocity meter, FP211 with the accuracy of 0.1 m/s. The corresponding water discharge was calculated subsequently. These values were averaged to represent the typical cross section and the hydraulic variables in the cutoff channel at the time of measurement in 2013. A cross section of the former channel located immediately upstream of the cutoff channel was surveyed using the standard geomorphological survey method (Harrelson et al., 1994) for both CT1 and CT2. At each survey point along the measured cross section, mean flow depth and velocity were measured as well. The slope of the cutoff channel was determined by measuring water level difference between its upstream and downstream ends using a theodolite and divided it by the length of the channel measured along the longitudinal direction. Sediment samples were collected from the river bed, point bar, and the inlet and outlet of the oxbow channel in CT1 and CT2, respectively from 2013 to 2016. These samples were subsequently analyzed to determine the particle size distribution and median grain size using manual sieving and a laser scattering particle analyzer (Mastersizer 2000). In 2016, repetitive measurements in a selected cross section of the cutoff and former channels in CT1 and CT2 were conducted, respectively, whereas in 2014, measurements were performed in CT1 only due to logistic limits and cross sections in CT2 were estimated subsequently based on field observation. In these two years, sediment plugs significantly raised the elevations of the inlet and outlet of the oxbow channel, such that flow in the former channel was either unable to or partly entered the oxbow channel for the measured flow.

The bank height and thickness of the upper mixture layer were measured at 32 locations along the concave bank of CT1 in 2017. Statistical analysis of these values indicated that on average the upper layer (Fig. 2) takes 30% of the bank height. Our preliminary test using a vane shear tester in July 2017 showed that the shear strength in this layer was at least twice higher than that in the lower layer. Therefore, we assumed that the water discharge reaching the bottom of the upper mixture layer is more effective in causing bank erosion than the bankfull discharge (Gautier et al., 2010) and selected this discharge for model simulation.

2.3. Analysis methods

Given that the artificial cutoffs in CT1 and CT2 did not significantly affect the sinuosity of the meander reach that contains the two bends, the slope of the former channel in CT1 and CT2 was calculated by obtaining the elevations of the beginning and ending points of the reaches including CT1 and CT2 and their longitudinal distances from the latest available satellite image (Google Earth), which turned out to be 0.0036. The relative frequency of each measured water discharge was determined using daily discharge (Q) data of the past 16 years between 1981 and 2014, which was estimated from the data available at the Zoige hydrological station in the middle of the Black River. These discharges were proportionally scaled to the study tributary based on their contributing areas. Given that the land cover of the region is nearly uniform (predominantly covered by peat), the linear conversion of the discharges was reasonable. Based on the curve established in the flood frequency analysis using the 16 peak discharges, recurrence interval (RI) of each measured water discharge was identified. For a given discharge series, the RI-Q relationship developed using different probability density functions, such as log-Pearson type III, extreme value distribution, and normal distributions, mainly shows the difference for large Q values with $RI > 10$. We developed this curve using the classic Weibull method (Chow et al., 1988). The RI values calculated using this method are slightly higher than those determined using a partial flood frequency analysis, but will not affect the relevant analysis in this study.

To characterize morphological changes of the channels after cutoffs, we constructed at-a-station hydraulic geometry (i.e., the relationships between a series of mean channel widths, depths, and flow velocities, and the associated discharges) for the measured cross sections in 2013, 2014, 2016. Each set of hydraulic geometry was determined using the reference reach spreadsheet (A Stream Module: Spreadsheet Tools for River Evaluation, Assessment and Monitoring, version 4.3L) (Macklenburg and Ward, 2004). In addition to cross section data, this method also requires information of the channel slope, particle size distribution of bed materials, and Manning's n ($m^{-1/3}$) of the channel. Values of the Manning's n ($m^{-1/3}$) were selected in terms of the classic categories (Arcement and Schneider, 1989), the particle size of bed materials, and our field observation. For the measured channels, values of n ranged between 0.01 and 0.06. The determined bankfull width and depth for the cutoff and former channel in CT1 and CT2 in 2013, 2014, and 2016 were subsequently used to examine the morphological changes of these channels. Although bankfull velocity of each channel may be determined from this method, it was not used in our analysis

Fig. 3. The two artificial ditches excavated in 2013.

because the associated bankfull discharge rarely occurred in CT1 and CT2 and hence was irrelevant to the channel adjustment in the study period. The developed hydraulic geometry was also used to determine the most effective discharges in CT1 and CT2 for the subsequent modeling analysis.

To further understand channel response to the artificial neck cutoff, we performed three-dimensional hydrodynamic simulation using MIKE3 Flow Model (DHI, 2008). Governing equations characterizing the flow field are based on the three-dimensional incompressible Reynolds-averaged Navier-Stokes model. Turbulence stresses are modelled by the Bousinesq approximation with assumed hydrostatic pressure. Vertical layers of the flow are divided using the σ-coordinate transformation. Horizontal eddy viscosity is calculated using the large eddy simulation equation while vertical eddy coefficient is determined using the k-ε turbulence closure model (Rodi, 1993). These equations are solved using the alternating direction implicit method. To account for hydraulic jump and drop, these equations are discretized using the finite volume method with high-order spatial discretization. In this method, the explicit upwind scheme is used to control the precision of calculation, and the time step is strict to meet the requirement that the Courant-Friedrich-Levy number should be < 0.8 (DHI, 2008).

Although modeling focused on hydrodynamic processes in CT1 and CT2 (Fig. 4), the spatial domain of the model was slightly larger than the lengths of the two bends to avoid boundary effect. The boundary and initial conditions of modeling were sufficiently characterized by three factors. The first was morphology of the simulated channel section, which was determined and estimated based on measured cross sections in 2013, 2014, and 2016. The second was mean channel slope, which was measured and set as 0.0036. The third was water discharges, which were the most effective ones determined using the established hydraulic geometry. In CT1, this discharge was 0.66 m^3/s for the former channel before and at the neck cutoff and 0.7 m^3/s for 2014 and 2016, respectively. In CT2, the four initial (effective) discharges were 0.47, 0.47, 0.93, and 0.7 m^3/s, respectively. These conditions formed eight simulation runs for CT1 and CT2, in which runs 1 and 5 were for the original former channel, runs 2 and 6 for the former channel at the time of neck cutoff, and runs 3, 4, 7, 8 for 2014 and 2016, respectively. Since these discharges were determined based on true values measured from the field, the model calibration using the actual flow data (Caamano et al., 2012; Feldens et al., 2015; Zavattero et al., 2016) was unnecessary. The original channel in CT1 was about 53 m long, which was divided by 27 cross sections (rectangle shape assumed) with a 2-m interval (L1-L27 in Fig. 4a). Furthermore, the 3-m-long cutoff channel at CT1 was divided by 11 cross sections with a 0.3-m interval (N1-N11 in Fig. 4a). The M-M section is the longitudinal profile of the cutoff channel, while the K-K section represents the transverse cross section in the upstream original channel. Similarly, in CT2, A1 to A27 are 27 cross sections, B1 to B11 are those within the cutoff channel, the C-C section is the corresponding longitudinal profile, and the D-D section is the cross section in the upstream original channel (Fig. 4b). To test the possible influence of the grid size used in the model on the simulated results, we selected three different grid sizes (a high, middle, and low resolution) for CT1 and CT2, respectively. The results showed that both spatial patterns and the ranges of simulated local velocities were similar among the three resolutions, indicating that selection of cell size has a negligible impact on model simulation. We then used the middle resolution, which contained 19,080 cells for CT1 and 23,668 cells for CT2, for all previously described eight runs. Since MIKE3 Flow Model is not capable of simulating sediment transport without field-measured sediment data, it was used in this study for illustrating spatially variable flow velocities in the three measurement years.

3. Results and analysis

3.1. Measured morphological changes of the cutoff channels

Immediately after ditch excavation in 2013, the cutoff channel in CT1 had a very low discharge, which only took about 6.2% of the total discharge in the former channel (Table 2). At this time, flow depth in the cutoff channel was about half of that in the former channel and the flow width was merely 7.9% of the former channel. However, flow velocity in the cutoff channel was even higher than that in the former channel. This high flow velocity for the given relatively small discharge was primarily caused by the significantly higher slope of the cutoff channel (i.e., 0.038) than that in the former channel (0.0036) as the result of ditch excavation. At this stage, the cutoff channel was subject to three morphologic and hydraulic conditions that led to its subsequent expansion. First, the relatively high flow velocity and channel slope suggested that the cutoff channel was subjected to relatively high stream power on average (Table 2). Second, the flow depth of the cutoff channel at the time of the measurement was only 38% of the bankfull depth, suggesting that the flow acts on the bank section composed of silt and clay that have relatively low shear strength. Third, the flow in both the cutoff and former channel had recurrence interval of 0.59 and 1.20, respectively (Table 2). Thus, the flow occurred in the cutoff channel tended to be more frequent.

In 2014, the measured discharge in the cutoff channel (i.e., 0.233 m^3/s) was about 50% of that in the former channel (i.e., 0.533 m^3/s), indicating that more flow in the former channel was diverted into the cutoff channel. This change was associated with the size expansion of the cutoff channel. Its width (i.e., 2.5 m) and depth (i.e., 0.15 m) reached 56% and 63% of those in the former channel at the same time, respectively. This expansion clearly resulted from bank erosion and channel incision in the past year. The measured discharge in the cutoff channel was still applied to the lower layer of the bank with silt and gravels because the flow depth was within 70% of the

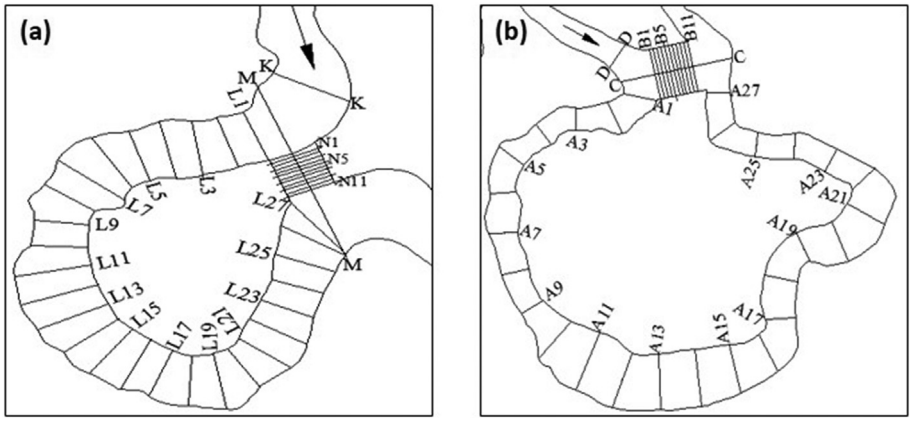

Fig. 4. Setup of cross sections in CT1 and CT2 for the three dimensional flow simulation. (a) CT1; (b) CT2.

Table 2
Morphologic and hydraulic values of all measured cross sections in CT1 and CT2.

Cross section ID	W_m (m)	H_m (m)	V_m (m/s)	Q_m (m^3/s)	*RI* (year)	Stream power (W m^{-2})
CT1_former_2013	4.208	0.289	0.558	0.661	1.199	5.7
CT1_cutoff_2013	0.332	0.189	0.648	0.041	0.593	46.0
CT1_former_2014	4.500	0.237	0.500	0.533	1.036	4.2
CT1_cutoff_2014	2.500	0.150	0.621	0.233	0.737	17.4
CT1_former_2016	5.280	0.315	0.605	1.005	1.772	6.7
CT1_cutoff_2016	5.490	0.277	0.661	1.005	1.772	16.1
CT2_former_2013	3.450	0.710	0.289	0.706	1.262	7.2
CT2_cutoff_2013	0.339	0.150	0.500	0.025	0.582	44.0
CT2_former_2016	3.440	0.780	0.349	0.941	1.648	9.7
CT2_cutoff_2016	6.282	0.435	0.344	0.941	1.648	21.0

bankfull depth, which was 0.41 m. Its recurrence interval (*RI*), which was 0.74, possibly suggested that similar discharges occurred relatively frequent each year. Thus, this type of discharges in the cutoff channel may be treated as one of the effective discharges that lead to persistent bank erosion and cantilever banks in the Zoige basin.

Two years later in 2016, our observation showed that the oxbow channel was completely disconnected from the former channel for the measured discharge, which was 1.0 m^3/s. Since the cutoff channel had evolved to the size similar to that of the former channel, both channels had similar mean hydraulic variables (Table 2). The relatively high *RI* (i.e., 1.77) suggested that most (if not all) discharges within a year bypassed the oxbow channel and the cutoff channel had become a part of the former channel.

In CT2, adjustment of the cutoff channel demonstrated similar characteristics. The original ditch only attracted about 4% of the total discharge in the former channel, while it had much higher mean flow velocity than that in the former channel (Table 2). The relatively low value of *RI* (i.e., 0.582) suggested that such discharge in the cutoff channel tended to occur more frequently and thus may cause more effective bank erosion and channel bed incision. In 2016, the discharge with *RI* of 1.65 was separated from the oxbow channel by the escalated sediment plugs in both inlet and outlet of the oxbow channel (based on our field observation), suggesting that the cutoff channel began to replace the oxbow channel and became a part of the former channel.

3.2. Bankfull morphological changes of the two cutoff channels and their interaction with the former channels

The first cutoff channel (CT1) had experienced uneven changes in the three years after the artificial connection. Within one year (i.e., from 2013 to 2014), the mean bankfull channel width (W_b) quickly expanded about 10 times from 0.38 to 3.40 m with a moderate increase of the mean bankfull depth (H_b) from 0.45 to 0.51 m (Table 3). The size of the channel cross section in the following two years (i.e., from 2014 to 2016) continuously increased, but with a decreased rate. Particularly, the value of W_b has increased from 3.40 to 6.40 m, while that of H_b has only increased from 0.51 to 0.87 m (Table 3). Although the second cutoff channel (CT2) had also changed significantly during the same three years, the trend of the change was different. In 2013, the manually excavated straight ditch was only 0.38 m wide and 0.45 m deep, which were the same as those of the CT1. Although a year later in 2014, its width and depth increased to 1.40 and 0.56 m, respectively (Table 3), the increase rate of W_b, was significantly lower than that of the CT1. In 2016, W_b increased considerably to 6.30 m, while H_b indeed decreased slightly to 0.52 m (Table 3). Starting from the similar artificial ditches, the two cutoff channels followed different paths of morphologic evolution.

Table 3
Bankfull morphology of all measured cross sections in CT1 and CT2.

Cross section ID	W_b (m)	H_b (m)	W_b/H_b
CT1_former_2013	4.1	0.41	10.00
CT1_former_2014	4.5	0.41	10.98
CT1_former_2016	5.4	0.37	14.59
CT1_cutoff_2013	0.38	0.45	0.84
CT1_cutoff_2014	3.40	0.51	6.67
CT1_cutoff_2016	6.40	0.87	7.36
CT1_upstream_2016	6.3	0.69	9.13
CT2_former_2013	3.5	0.84	4.17
CT2_former_2014	3.5	0.93	3.76
CT2_former_2016	3.5	0.96	3.65
CT2_cutoff_2013	0.38	0.45	0.84
CT2_cutoff_2014	1.4	0.56	2.50
CT2_cutoff_2016	6.3	0.52	12.12
CT2_downstream_2016	4.37	0.57	7.67

In CT1, the narrow, but deep ditch was characterized by a small *W/H* value (0.84), which substantially increased to 6.67 one year later (i.e., 2014) and slightly augmented to 7.36 in 2016 (Fig. 5a). In the same period, the former channel immediate upstream of the cutoff channel showed a continuous increase in size represented by a gradual increase of the *W/H* ratio from 10 in 2013 to 14.59 in 2016. However, a cross section upstream of the artificial cutoff channel in CT1 (i.e., 'upstream' in Fig. 5a) had a *W/H* ratio of 9.13 in 2016, which was close to that of the cross section immediately upstream of the cutoff channel in 2013. Given that this cross section was not directly affected by the evolution of the cutoff channel, the different *W/H* values of the two cross sections along the former channel suggested that the morphology of the former channel immediately upstream of the cutoff channel was affected by the evolution of the cutoff channel in the three post-cutoff years. The much less difference of W/H ratios between this upstream and cutoff channels suggested that in 2016, the cutoff channel had comparable size to that of the former channel.

In CT2, the *W/H* ratio of the cutoff channel increased from 2013 to 2016, but with more regular rates (Fig. 5b). Although in 2014, the *W/H* value (i.e., 2.5) was lower than that (i.e., 6.67) in CT1, it was much higher in 2016 (i.e., 12.12) than that in CT1 (i.e., 7.36). Comparing with this increasing trend, the *W/H* value in the former channel immediately downstream of the cutoff channel demonstrated a marginally decreasing trend (Fig. 5b), suggesting that the evolution of the cutoff channel was irrelevant to that of the former channel. The higher *W/H* ratio in the downstream cross section than that in the former channel showed localized impact of the cutoff channel on its nearby sections. Clearly, the two cutoff channels interacted with the former channel differently during their evolution in the three years after the artificial cutoff. Since the slopes of the cutoff channel in CT2 were generally higher than those in CT1, the different interaction might be related to the different slopes of the two cutoff channels. Although the detailed evolution paths may be different, the cutoff channel in both bends may adjust itself to the former channel both hydraulically and morphologically in the three-year period immediately after the cutoff.

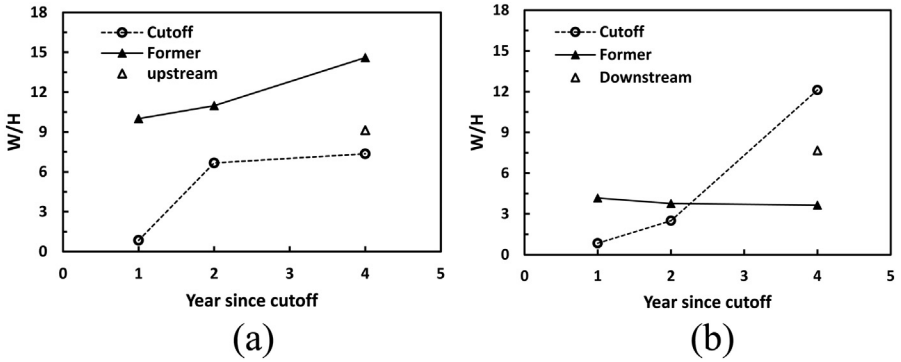

Fig. 5. Temporal trends of width/depth ratio for both the cutoff and former channels. (a) CT1, (b) CT2. 'Cutoff' denotes the cutoff channel; 'Former' stands for the former channel before the artificial cutoff; 'upstream' means a cross section immediately upstream of the original bend (i.e., CT1 or CT2).

Table 4
Hydraulic characteristics of the simulated channel in CT1 and CT2.

Location	Year	Water depth (m)	Width-depth ratio	Diversion angle (°)	Discharge (m^3/s)	Discharge diversion ratio (%)
CT1	2013	0	/	68	0	0
	2014	0.25	13.60	35	0.67	95.7
	2016	0.16	36.88	30	0.69	98.6
CT2	2013	0	/	80	0	0
	2014	0.32	4.38	48	0.65	69.9
	2016	0.20	31.5	32	0.69	98.6

3.3. Three-dimensional hydrodynamic simulation in CT1

Simulated width/depth ratios showed a similar increasing trend from 2014 to 2016 (Table 4). In 2013, the discharge entered the artificial ditch (see Table 2) was less than the minimum discharge MIKE3 would output, which is 0.05 m^3/s. Thus, the reported discharge was zero (Table 4), though the effect of the actual discharge was considered in the model. Comparing velocity distribution of the former channel in CT1 before and after the excavation of the artificial ditch in 2013 indicated that it was not significantly affected by the ditch. This may be because only about 6% of the mainstream discharge was diverted into the ditch (Table 4). In the former channel, the two-dimensional (2D) flow contour of CT1 showed typical bend flow distribution (Blanckaert, 2010; Blanckaert and Graf, 2001; Termini and Piraino, 2011). Higher velocity clusters emerged sporadically along the bend with more toward the outer bank (Fig. 6a). Vertically, higher velocities remained in the zone near the right bank and above the channel bed with a secondary circular flow in cross sections both upstream of the inlet and downstream of the outlet of the CT1 bend (Fig. 6b), showing a regular hydrodynamic pattern around a meandering bend –that is, channel migration is controlled more by lateral erosion than bed incision.

In 2014, velocities in the cutoff channel and its upstream and downstream sections were significantly higher than those in the oxbow channel (Fig. 6c). This was consistent with the prediction that about 96% of the total discharge was diverted into the cutoff channel in 2014 (Table 4), which was also in line with our field observation (Table 2). In the cutoff channel, high-velocity cells with the magnitudes much greater than those in the artificial ditch in 2013 followed a curve along the right (outer) bank (Fig. 6c). The associated cross-sectional flow field further showed localized high velocity toward the right bank and the intensified circular flow due to velocity difference in the lateral direction (Fig. 6d). These localized velocity patterns strongly suggested that the cutoff channel of CT1 experienced more bed and bank erosion from 2013 to 2014, which explained the widened channel compared with its size in 2013. At the same time, localized high-velocity was also developed in both the upstream and downstream cross sections near the cutoff channel, suggesting that intensified bank erosion at this time had extended outside of the cutoff channel.

Two years later in 2016, velocity distribution in both the cutoff and former channels remained similar patterns to those in 2014 (Fig. 6c and e). Apparently, the intensities of the localized velocities were reduced with locus of high velocities shifted to the center of the representative cross section in the cutoff channel (Fig. 6e and f). These velocity patterns explained the continuously enlarged size of the cross sections in both the cutoff and former channels but at a less degree, which supported the further increased width/depth ratio (Table 3) and essentially

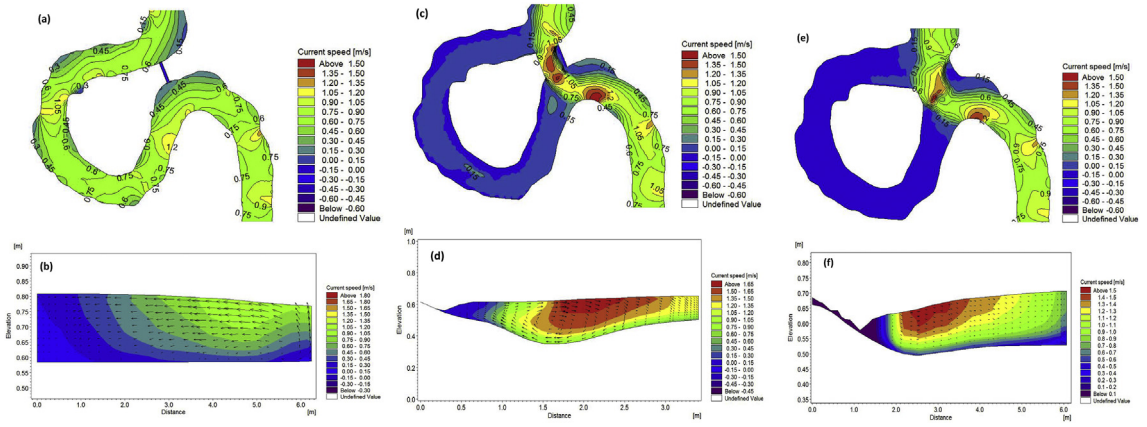

Fig. 6. Results of the three-dimensional simulation for CT1. (a) the plan view in 2013, (b) a representative cross sectional flow field in the middle of the cutoff channel in 2013, (c) the plan view in 2014, (d) a representative cross sectional flow field in the middle of the cutoff channel in 2014, (e) the plan view in 2016, (f) a representative cross sectional flow field in the middle of the cutoff channel in 2016.

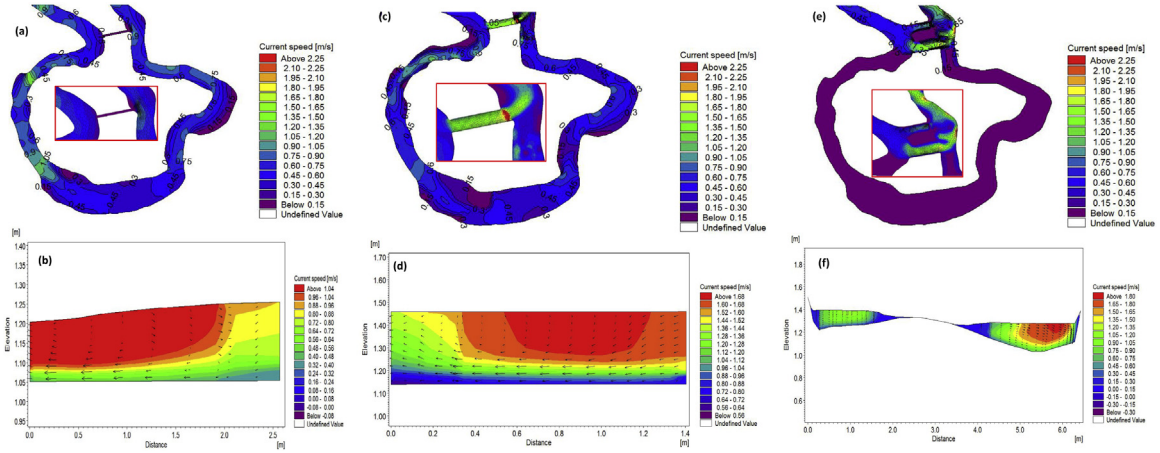

Fig. 7. Results of the three-dimensional simulation for CT2. (a) the plan view in 2013, (b) a representative cross sectional flow field in the middle of the cutoff channel in 2013, (c) the plan view in 2014, (d) a representative cross sectional flow field in the middle of the cutoff channel in 2014, (e) the plan view in 2016, (f) a representative cross sectional flow field in the middle of the cutoff channel in 2016.

all of the total discharge began to flow into the cutoff channel (Table 4). In 2014, velocities in the oxbow channel became almost zero, while in 2016, they were all zero (Fig. 6b and d). Again, these simulated results were consistent with the observed sediment plug in both inlet and outlet of the oxbow channel in 2016. It should be noted that these velocity changes were accompanied by the continuous decrease of diversion angle from 80 in 2013 to 32 in 2016 (Table 4).

3.4. Three-dimensional hydrodynamic simulation in CT2

In 2013, similar to that in CT1, the neck cutoff in CT2 did not change the velocity distribution in the former channel except increased local velocity around the inlet of the artificial ditch and velocity distribution in an upstream cross section of the former channel was also relatively dispersed with higher values spreading in the middle and on the left (Fig. 7a and b). Although CT1 and CT2 had a similar cutoff ratio and ditch morphology (Table 1), CT2 had higher diversion angle (i.e., an intersection angle between the former and cutoff channel), which only led about 3.6% of the total discharge to move into the ditch. These differences might set up a different adjustment path for the cutoff channel of CT2 from that of CT1.

One year later in 2014, velocities in the cutoff channel were generally higher than those in the former channel, which was highlighted by a transverse belt of very high velocities near its downstream end (Fig. 7c). The representative cross-sectional flow field (Fig. 7d) indicated that velocities were less concentrated and more symmetric than those in CT1, suggesting less intensity of channel bank erosion than that in CT1. These features of local velocities provided hydraulic reasons for the less expanded size of the cutoff channel in CT2 compared with that in CT1. The lower percentage of the diverted discharge (i.e., about 70%) from the total in CT2 (Table 4) might be related to the relatively high diversion angle compared with that in CT1, though it still reduced from 80° in 2013 to 48° in 2014. Because there were still about 30% of the total discharges entering the oxbow channel, it had not been isolated from the former channel yet with velocities mainly ranging between 0.30 and 0.60 m/s (Fig. 7c).

In 2016, both velocity distribution and morphology of the cutoff channel were different from those in CT1 (Fig. 7e). High velocity cluster moved to the downstream end of the enlarged cutoff channel, showing a tendency of developing a new bend in the cutoff channel. Furthermore, local velocities were divided by a central zone of zero velocity, which may reflect a developed central bar, into relatively uniform, but small velocities along the left bank and much higher, clustered velocities next to the right bank. This pattern was supported by a representative cross-sectional flow field within the cutoff channel (Fig. 7f) where the cross section was literally split into two sections with the right dominated by the localized velocities clustered near the right bank and the left characterized by the almost evenly distributed velocities in a large part. This strong localized velocity cluster explained the continuous erosion from 2014 to 2016 that led to the almost linear increase of the width/depth ratio observed in the field (Table 3). The consequence of this process was the further reduced diversion angle (from 48° in 2014 to 32° in 2016) and almost complete alteration of the total discharge into the cutoff channel (99%), which was consistent with our field observation (Table 2). At this stage, the oxbow channel was essentially disconnected from the former channel, which may be reflected by the general zero velocity predicted by the model (Fig. 7e). The development of a central bar presented in the cutoff channel of CT2 was similar to that reported by Hooke (1995b).

4. Discussion

4.1. Different evolutional paths of the two cutoff channels and their controlling factors

Status of meander evolution is primarily controlled by channel gradient, stream power, erodibility of channel bed and banks, and sediment supply (Hickin and Nanson, 1984; Larsen et al., 2006; Nicoll and Hickin, 2010; Timar, 2003). Although slopes of cutoff channels for CT1 and CT2 were different from 2013 to 2016, they both decreased fast during the three-year study period (Fig. 8a). Assuming the decreasing trend continues, it will take about one to two years for the slopes approaching the average slope of the reach (i.e., 0.036). Unit stream power (ω) in the cutoff channel of both CT1 and CT2 decreased continuously from 2013 to 2016, while that in the former channel remained roughly unchanged during the same period (Fig. 8b). The much higher ω value of the cutoff channel than that of the former channel in 2013 encouraged the size increase of the cutoff channel for both CT1 and CT2. In 2016, however, the decreased ω value in the cutoff channel suggested the reduced rate of change in size, though it would continue as this value was still higher than that in the former channel. Information about sediment supply during the study period was not available due to the difficulty of in situ measurement. Yet, bed materials of the cutoff channel were coarsened from 2013 (D_{50} = 4.6 mm) to 2016 (D_{50} = 10.0 mm), suggested that sediment supply was limited. Even though, the observed prompt sediment plug one year after the artificial cutoff implied that sufficient amount of sediment was supplied to CT1 and CT1 each year to initiate sediment deposition in the oxbow channel. Similar characteristics of these three factors in CT1 and CT2 determined that both cutoff channels gained comparable sizes to the

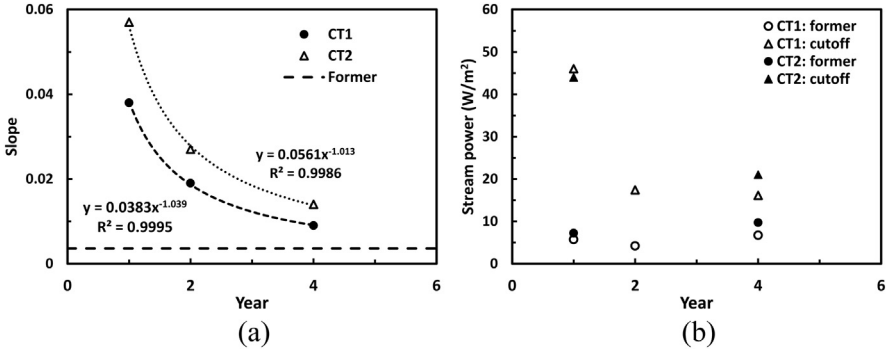

Fig. 8. Temporal changes of slope and unit stream power in the cutoff and former channels. (a) slope, (b) unit stream power.

former channel in the third year after the cutoff.

Nonetheless, the two cutoff channels followed two distinct evolution paths during the three-year period, which may be highlighted in two aspects. First, in the year after their creation, the cutoff channel in CT1 experienced much greater degrees of channel enlargement than that in CT2. This difference was obviously caused by much higher bank erosion in the cutoff channel of CT1, but could not be explained by the average hydraulic variable, unit stream power, because this variable was similar in both cutoff channels in 2013 (Fig. 8b). What lends to the explanation was the stronger localized cluster of high velocities next to the right bank of the CT1 channel than that in the CT2 channel (Figs. 6b and 7b), which may trigger much higher localized bank erosion in the cutoff channel of CT1. The high localized velocity cluster may be ascribed to the initial diversion angle, which was smaller in CT1 (68°) than in CT2 channel (80°) in 2013 (Table 4). Flows with a smaller diversion angle were easier to enter the channel with higher local velocities concentrated on the right bank, resulting in different local patterns of velocity distribution. This velocity difference also generated a curved flow path in the CT1 channel (Fig. 6c) and a relatively straight one in the CT2 channel (Fig. 7c). Consequently, in 2014, the cross-sectional flow field in the middle of the CT1 channel had an inclined water surface, whereas that in the CT2 channel had a horizontal one (Figs. 6d and 7d), which was further confirmed by the higher diversion angle in the CT1 than that in the CT2 in 2014 (Table 4). Therefore, diversion angle is a control factor for the adjustment of a cutoff channel (Konsoer and Richards, 2016) besides its role in controlling the degree of sediment deposition in the oxbow channel caused by chute or neck cutoff (Constantine et al., 2010a, 2010b; Ishii and Hori, 2016; Zinger et al., 2011).

Second, from 2014 to 2016, the flow pattern of the cutoff channel in CT1 did not change obviously (Fig.6c and e), while that in CT2 evolved significantly (Fig. 7c and e). The generally greater intensity of the concentrated high velocities of CT2 in 2014 (Fig. 7c) induced higher bank erosion rates, which led to not only the subsequent increase of channel width, but also deposition along the channel center from its middle to downstream end (Fig. 7c and e). As such, the flow pattern in the cutoff channel of CT2 was completely different from that in CT1 in 2016 (Figs. 6e and 7e).

Given that the lower portion of the bank, which had clay, silt, and gravels without the protection of vegetation roots (Fig. 2), is more erodible, higher degree of bank erosion occurred in the lower than in the top portion, finally resulting in more soils lost in the lower sections of the banks and causing the overhang of the upper part of the banks. Once its weight reached the threshold of the balance, it collapsed as a slump block and then gradually swept out (Parker et al., 2011; Pizzuto, 1984). This process of cantilever bank failure was evidenced by our field observation in 2013–2017 when we noticed individual bank bodies slumped or fell on the channel bed in the cutoff channels. The existence of slump blocks explained the formation of the bifurcated flow paths in the CT2 channel in 2016 (Fig. 7e and f). Thus, intensity of bank failure is an additional factor influencing the trend of channel adjustment.

It should be noted that the simulated distributions of flow depths and velocities in Sections 3.3 and 3.4 were not validated because measuring them in situ in the Qinghai-Tibet Plateau is extremely difficult, if not impossible. The use of a simplified rectangular cross sections also introduced possible errors in the simulated results. Nonetheless, these simulation results were used to show the hydrodynamic characteristics of the flows, rather than to predict the exact values of the distributed flow depths and velocities in the simulated channels.

4.2. Comparison with natural cutoff channels

Evolution of meandering channels after the neck cutoff in this study shared three common characteristics with that of two meandering rivers in the northwest England (Hooke, 1995b). First, channel morphology changed most in the first three years (with variable rates) because the shape and size of the cutoff channels in 2016 were similar to those of the previous channels; Second, the upstream section of the cutoff channel experienced increased erosion; Third, in both the entrance and exit of the oxbow channel, sediment plug happened rapidly, such that a great proportion or almost all of the flow discharges were diverted to the cutoff channel only one year later, accelerating the disconnection of the oxbow channel to the former one. Yet, the three neck cutoffs in the White River within Arkansas, USA (Konsoer and Richards, 2016) provided opposite cases. In these cutoff channels that represented different evolution stages after neck cutoffs, their upstream channel segments experienced little or limited local erosion, which was insufficient to enlarge the upstream segments significantly. Consequently, a significant proportion of flows continued to enter the oxbow channel. Based on results from their field investigations, it may be concluded that evolution of the channel due to neck cutoff is generally controlled by the increased channel gradient and unit stream power compared with those in the corresponding former channels, as well as enhanced flow velocities concentrated on local areas of the cutoff banks. However, these factors are insufficient to explain the different evolutional paths of the cutoff channel between CT1 and CT2 in this study and the high hydrological connection between the cutoff and former channels in Konsoer and Richards (2016). We noticed from the planform of the cutoff bends in these three rivers and those in France (Citterio and Piegay, 2009; Piegay et al., 2000) that the diversion angle in the White River, USA was generally high, while decreased continuously in both bends of the river within the Zoige basin (i.e., this study) and a river in the northwest England (i.e., Figs. 5 and 7 in Hooke, 1995b). Since the diversion angle reflects the orientation of the former and oxbow channels, which influences sedimentation in the oxbow channel (Citterio and Piegay, 2009), we think this factor is particularly important in controlling the evolution paths of a cutoff channel.

5. Conclusions

Meandering rivers as tributaries of the Upper Yellow River in the Zoige basin are dominated by neck cutoffs. Yet, little has been known about the processes of subsequent channel adjustment after cutoffs, mainly because of the difficulty of obtaining field-measured data in this high-elevation area. This study served as an attempt of exposing these processes. By excavating ditches along the narrowest neck of two meandering bends, we artificially triggered neck cutoff in two highly convoluted bends in the upper Maiqu River of the Zoige basin on July 5 and 6, 2013. Consecutive in situ measurements of channel morphology and flow hydraulics in 2013, 2014, 2016, and 2017 provided field data for understanding the nature of channel adjustment after neck cutoff, which was supplemented by our hydraulic-geometry analysis and three-dimensional simulation. We found that cutoff channels expanded quickly and became 'mature' in three years. In general, adjustment of the cutoff channels was mainly controlled by channel gradient, unit stream power, and bank strength. In particular, the specific path of channel evolution was primarily determined by the diversion angle. Furthermore, we revealed that the unique process of controlling bank erosion, the cantilever bank failure, is the dominant process influencing the distribution of riffles and pools within the cutoff channel of the meandering river in the Zoige basin. These features of channel adjustment are not completely consistent with those in two other meandering rivers of different sizes and physical settings in northwest England and Arkansas, USA, suggesting the complexity of the processes controlling channel adjustment after neck cutoff and calling for more field-based study for further understanding this complexity.

Acknowledgements

This study has been supported by the National Natural Science Foundation of China (91547112, 91647204, 91647118, and 51709020), and the Open Project of State Key Laboratory of Plateau Ecology and Agriculture, Qinghai University, China (2017-KF-01), the Project of Qinghai Science & Technology Department, China (2016-ZJ-Y01, 2016-HZ-802), Natural Science Foundation of Hunan Province, China (2018JJ3547), and Changsha Science and Technology Plan Project, China (kq1701075). The second author was also partially supported by the Appleby-Mosher fund of Maxwell School of Citizenship and Public Affairs, Syracuse University. We thank Professor Zhaoyin Wang and Professor Xuyue Hu for their support of our field survey in 2013-2014 and in 2016-2017, respectively. We also thank Xiongdong Zhou, Liqun Lv, Lijian Qi, Jing Liu, and Xiang Li for their field assistance and Xinyu Wu for partly helping us process data. Finally, we like to thank Kory Konsoer and another reviewer for providing thoughtful critiques and suggestions.

References

Arcement, G.J., Schneider, V.R., 1989. Guide for Selecting Manning's Roughness Coefficients for Natural Channels and Flood Plains. United States Geological Survey Water-supply Paper, pp. 2339.

Aslan, A., Autin, W.J., Blum, M.D., 2005. Causes of river avulsion: insights from the late Holocene avulsion history of the Mississippi River, USA. J. Sediment. Res. 75, 650–664.

Blanckaert, K., 2010. Topographic steering, flow recirculation, velocity redistribution, and bed topography in sharp meander bends. Water Resour. Res. 46, W09506. https://doi.org/10.1029/2009WR008303.

Blanckaert, K., Graf, W.H., 2001. Mean flow and turbulence in open-channel bend. J. Hydraul. Eng. 127, 835–847.

Braudrick, C.A., Dietrich, W.E., Leverich, G.T., Sklar, L.S., 2009. Experimental evidence for the conditions necessary to sustain meandering in coarse-bedded rivers. In: Proceedings of the National Academy of Sciences of the United States of America. 106. pp. 16936–16941.

Bray, D.I., Cullen, A.J., 1976. Study of artificial cutoffs on gravel-bed rivers. In: Rivers '76 Symposium on Inland Waterways for Navigation, Flood Control and Water Diversions. 2. pp. 1399–1417.

Brice, J.C., 1984. Planform properties of meandering rivers. In: Elliot, C.M. (Ed.), River Meandering. AmericanS ocietyo f Civil Engineers, New York, pp. 1–15.

Caamano, D., Goodwin, P., Buffington, J.M., 2012. Flow structure through pool-riffle sequences and a conceptual model for their sustainbility in gravel-bed rivers. River Res. Appl. 28, 377–389. https://doi.org/10.1002/rra.1463.

Camporeale, C., Perona, P., Porporato, A., Ridolfi, L., 2005. On the long-term behavior of meandering rivers. Water Resour. Res. 41.

Camporeale, C., Perona, P., Porporato, A., Ridolfi, L., 2007. Hierarchy of models for meandering rivers and related morphodynamic processes. Rev. Geophys. 45, RG1001.

Camporeale, C., Perucca, E., Ridolfi, L., 2008. Significance of cutoff in meandering river dynamics. J. Geophys. Res. Earth Surf. 113.

Chow, V.T., Maidment, D.R., Mays, L.W., 1988. Applied Hydrology. McCraw-Hill Book Company, New York.

Citterio, A., Piegay, H., 2009. Overbank sedimentation rates in former channel lakes: characterization and control factors. Sedimentology 56, 461–482.

Constantine, J.A., Dunne, T., 2008. Meander cutoff and the controls on the production of oxbow lakes. Geology 36, 23–26.

Constantine, J.A., Dunne, T., Piegay, H., Kondolf, G.M., 2010a. Controls on the alluviation of oxbow lakes by bed-material load along the Sacramento River, California. Sedimentology 57, 389–407.

Constantine, J.A., McLean, S.R., Dunne, T., 2010b. A mechanism of chute cutoff along large meandering rivers with uniform fl oodplain topography. Geol. Soc. Am. Bull. 122, 855–869. https://doi.org/10.1130/B26560.1.

Constantine, J.A., Dunne, T., Ahmed, J., Legleiter, C., Lazarus, E.D., 2014. Sediment supply as a driver of river meandering and floodplain evolution in the Amazon Basin. Nat. Geosci. 7, 899–903.

Deptuck, M.E., Sylvester, Z., Pirmez, C., O'Byrne, C., 2007. Migration-aggradation history and 3-Dseismic geo-morphology of submarine channels in the Pleistocene Benin-major Canyon, western Niger Delta slope. Mar. Pet. Geol. 24, 406–433.

DHI, 2008. MIKE 3 Flow Model FM. Denmark, Horsholm.

Ebisemiju, F.S., 1993. The planimetric and geometric-properties of the channel bends of low-energy streams in a forested humid tropical environment, southwestern Nigeria. J. Hydrol. 142, 319–335.

Eekhout, J.P.C., Hoitink, A.J.F., 2015. Chute cutoff as a morphological response to stream reconstruction: the possible role of backwater. Water Resour. Res. 51, 3339–3352.

Erskine, W.D., 1992. Channel response to large-scale river training works - Hunter River, Australia. Regul. Rivers Res. Manag. 7, 261–278.

Erskine, W., Mcfaden, C., Bishop, P., 1992. Alluvial cutoffs as indicators of former channel conditions. Earth Surf. Process. Landf. 17, 23–37.

Feldens, P., Diesing, M., Schwarzer, K., Heinrich, C., Schlenz, B., 2015. Occurrence of flow parallel and flow transverse bedforms in Fehmarn Belt (SW Baltic Sea) related to the local palaeomorphology. Geomorphology 231, 53–62.

Finnegan, N.J., Dietrich, W.E., 2011. Episodic bedrock strath terrace formation due to meander migration and cutoff. Geology 39, 143–146.

Fisk, H.N., 1944. Geological Investigations of the Alluvial Valley of the Lower Mississippi River, Mississippi River Commission. U.S. Army Corps of Engineers, Vicksburg, Mississippi.

Fisk, H.N., 1947. Fine Grained Alluvial Deposits and their Effects on Mississippi River activity. Mississippi River Commission, Vicksburg, MS.

Frascati, A., Lanzoni, S., 2009. Morphodynamic regime and long-term evolution of meandering rivers. J. Geophys. Res. Earth Surf. 114.

Frascati, A., Lanzoni, S., 2010. Long-term river meandering as a part of chaotic dynamics? A contribution from mathematical modeling. Earth Surf. Process. Landf. 35, 791–802.

Friedkin, J.F., 1945. A Laboratory Study of Meandering of Alluvial Rivers, Mississippi River Commission. U.S. Waterways Experiment Station, Vicksburg, Mississippi.

Fuller, I.C., Large, A.R.G., Milan, D.J., 2003. Quantifying channel development and sediment transfer following chute cutoff in a wandering gravel-bed river. Geomorphology 54, 307–323.

Gautier, E., et al., 2007. Temporal relations between meander deformation, water discharge and sediment fluxes in the floodplain of the Rio Beni (Bolivian Amazonia). Earth Surf. Process. Landf. 32, 230–248.

Gautier, E., et al., 2010. Channel and floodplain sediment dynamics in a reach of the tropical meandering Rio Beni (Bolivian Amazonia). Earth Surf. Process. Landf. 35, 1838–1853.

Gay, G.R., et al., 1998. Evolution of cutoffs across meander necks in Powder River, Montana, USA. Earth Surf. Process. Landf. 23, 651–662.

Ghinassi, M., 2011. Chute channels in the Holocene high-sinuosity river deposits of the Firenze plain, Tuscany, Italy. Sedimentology 58, 618–642.

Gilvear, D., Winterbottom, S., Sichingabula, H., 2000. Character of channel planform change and meander development: Luangwa River, Zambia. Earth Surf. Process. Landf. 25, 421–436.

Grenfell, M., Aalto, R., Nicholas, A., 2012. Chute channel dynamics in large, sand-bed meandering rivers. Earth Surf. Process. Landf. 37, 315–331.

Guneralp, I., Marston, R.A., 2012. Process-form linkages in meander morphodynamics: bridging theoretical modeling and real world complexity. Prog. Phys. Geogr. 36, 718–746.

Guneralp, I., Rhoads, B.L., 2009. Empirical analysis of the planform curvature-migration relation of meandering rivers. Water Resour. Res. 45, W09424.

Guneralp, I., Abad, J.D., Zolezzi, G., Hooke, J., 2012. Advances and challenges in meandering channels research. Geomorphology 163, 1–9.

Gutierrez, R.R., Abad, J.D., 2014. On the analysis of the medium term planform dynamics of meandering rivers. Water Resour. Res. 50, 3714–3733.

Hager, W.H., 2003. Fargue, founder of experimental river engineering. J. Hydraul. Res. 41, 227–233.

Han, B., Endreny, T., 2014. Detailed river stage mapping and head gradient analysis during meander cutoff in a laboratory river. Water Resour. Res. 50, 1689–1703. https://doi.org/10.1002/2013WR013580.

Harrelson, C.C., Rawlins, C.L., Potyondy, J.P., 1994. Stream Channel Reference Sites: An Illustrated Guide to Field Technique. United States Department of Agriculture, Forest Service, Rocky Mountain Forest and Range Experiment Station, Fort Collins, Colorado.
Hauer, C., Habersack, H., 2009. Morphodynamics of a 1000-year flood in the Kamp River, Austria, and impacts on floodplain morphology. Earth Surf. Process. Landf. 34, 654–682.
Hickin, E.J., Nanson, G.C., 1984. Lateral migration rates of river bends. J. Hydraul. Eng. ASCE 110, 1557–1567.
Hooke, J.M., 1984. Changes in river meanders - a review of techniques and results of analyses. Prog. Phys. Geogr. 8, 473–508.
Hooke, J.M., 1995a. Processes of channel planform change on meandering channels in the UK. In: Gurnell, A., Petts, G.E. (Eds.), Changing River Channels. John Wiley & Sons, Ltd., Chichester, UK, pp. 87–115.
Hooke, J.M., 1995b. River channel adjustment to meander cutoffs on the River Bollin and River Dane, northwest England. Geomorphology 14, 235–253.
Hooke, J.M., 2004. Cutoffs galore!: occurrence and causes of multiple cutoffs on a meandering river. Geomorphology 61, 225–238.
Hooke, J.M., 2013. River meandering. In: Shroder, J.F.E.-i.-c., Wohl, E.V.E. (Eds.), Treatise on Geomorphology Vol 9, Fluvial Geomorphology. Academic Press, San Diego, pp. 260–288.
Hooke, J.M., Redmond, C.E., 1992. Causes and nature of river planform change. In: Billi, P., Hey, R.D., Thorne, C.R., Tacconi, P. (Eds.), Dynamics of Gravel-Bed Rivers. Wiley, Chichester, pp. 549–563.
Howard, A.D., 1992. Modeling channel migration and floodplain sedimentation in meandering streams. In: Carling, P.A., Petts, G.E. (Eds.), Lowland Floodplain Rivers: Geomorphological Perspectives. John Wiley & Sons Ltd., Chichester, UK, pp. 1–41.
Howard, A.D., 2009. How to make a meandering river. Proc. Natl. Acad. Sci. U. S. A. 106, 17245–17246.
Howard, A.D., Knutson, T.R., 1984. Sufficient conditions for river meandering - a simulation approach. Water Resour. Res. 20, 1659–1667.
Hudson, P.F., Kesel, R.H., 2000. Channel migration and meander-bend curvature in the lower Mississippi River prior to major human modification. Geology 28, 531–534.
Ikeda, S., Parker, G., Sawai, K., 1981. Bend theory of river meanders. 1. Linear development. J. Fluid Mech. 112, 363–377.
Ishii, Y., Hori, K., 2016. Formation and infilling of oxbow lakes in the Ishikari lowland, northern Japan. Quat. Int. 397, 136–146. https://doi.org/10.116/j.quaint.2015.06.016.
Knighton, D., 1998. Fluvial Forms & processes, A New Perspective. Arnold, London.
Konsoer, K.M., Richards, G., 2016. Planform evolution of neck cutoffs on elongate meander loops, White River, Arkansas, USA. In: Constantinescu, G., Garcia, M., Hanes, D. (Eds.), River Flow 2016. Taylor & Francis Group, Boca Raton.
Larsen, E.W., Fremier, A.K., Girvetz, E.H., 2006. Modeling the effects of variable annual flow on river channel meander migration patterns, Sacramento River, California, USA. J. Am. Water Resour. Assoc. 42, 1063–1075.
Le Coz, J., et al., 2010. Morphodynamics of the exit of a cutoff meander: experimental findings from field and laboratory studies. Earth Surf. Process. Landf. 35, 249–261.
Lewis, G.W., Lewin, J., 1983. Alluvial cutoffs in Wales and the Borderlands. Int. Assoc. Sedimentol. Spec. Publ. 6, 145–154.
Li, Z.W., Yu, G.A., Brierley, G., Wang, Z.Y., Jia, Y.H., 2017. Migration and cutoff formation of meanders in hyper-arid environments of the middle and lower Tarim River, Northwestern China. Geomorphology 276, 116–124.
Lonsdale, P., Hollister, C.D., 1979. Cut-offs at an abyssal meander south of Iceland. Geology 7, 597–601.
Luchi, R., Zolezzi, G., Tubino, M., 2011. Bend theory of river meanders with spatial width variations. J. Fluid Mech. 681, 311–339.
Macklenburg, D.E., Ward, A., 2004. STREAM modules: spreadsheet tools for river evaluation, assessment and montoring. In: Conference Proceedings for the ASAE Specialty Conference “Self-sustaining Solutions for Streams, Wetlands, and Watersheds”, St. Paul, Minnesota, https://doi.org/10.1061/41173(414)265.
Matsubara, Y., et al., 2015. River meandering on Earth and Mars: a comparative study of Aeolis Dorsa meanders, Mars and possible terrestrial analogs of the Usuktuk River, AK, and the Quinn River, NV. Geomorphology 240, 102–120.
Micheli, E.R., Larsen, E.W., 2011. River channel cutoff dynamics, sacramento river, california, USA. River Res. Appl. 27, 328–344.
Morais, E.S., Rocha, P.C., Hooke, J., 2016. Spatiotemporal variations in channel changes caused by cumulative factors in a meandering river: the lower Peixe River, Brazil. Geomorphology 273, 348–360.
Nanson, G.C., Hickin, E.J., 1983. Channel migration and incision on the beatton river. J. Hydraul. Eng. ASCE 109, 327–337.
Nicoll, T.J., Hickin, E.J., 2010. Planform geometry and channel migration of confined meandering rivers on the Canadian prairies. Geomorphology 116, 37–47.
Nicoll, T., Brierley, G.J., Yu, G.A., 2013. A broad overview of landscape diversity of the Yellow River source zone. J. Geogr. Sci. 23, 793–816.
Ollero, A., 2010. Channel changes and floodplain management in the meandering middle Ebro River, Spain. Geomorphology 117, 247–260.
Pan, C.S., Shi, S.C., Duan, W.Z., 1978. A study of the channel development after the completion of artificial cutoffs in the Middle Yangtze River. Sci. Sinica 21, 783–804.
Pang, B.D., 1986. An investigation about natural cutoffs on the lower reaches of the Wei River after the construction of the Sanmenxia Reservoir. J. Sediment. Res. 4, 37–49 (in Chinese).
Parker, G., et al., 2011. A new framework for modelling the migration of meandering rivers. Earth Surf. Process. Landf. 36, 70–86.
Peakall, J., Ashworth, P.J., Best, J.L., 2007. Meander-bend evolution, alluvial architecture, and the role of cohesion in sinuous river channels: a flume study. J. Sediment. Res. 77, 197–212.
Perucca, E., Camporeale, C., Ridolfi, L., 2005. Nonlinear analysis of the geometry of meandering rivers. Geophys. Res. Lett. 32, L03402.
Piegay, H., et al., 2000. Channel instability as a control on silting dynamics and vegetation patterns within perifluvial aquatic zones. Hydrol. Process. 14, 3011–3029.
Pizzuto, J.E., 1984. Bank erodibility of shallow sandbed streams. Earth Surf. Process. Landf. 9, 113–124.
Rodi, W., 1993. Turbulence models and their application in hydraulics-a state of the art review, third ed. Balkema, Rotterdam, The Netherlands.
Schumm, S.A., 1977. The Fluvial System. Wiley-Interscience, New York.
Seminara, G., Zolezzi, G., Tubino, M., Zardi, D., 2001. Downstream and upstream influence in river meandering. Part 2. Planimetric development. J. Fluid Mech. 438, 213–230.
Smith, L.M., Winkley, B.R., 1996. The response of the Lower Mississippi River to river engineering, Engineering. Geology 45, 433–455.
Stolum, H.H., 1996. River meandering as a self-organization process. Science 271, 1710–1713.
Stolum, H.H., 1998. Planform geometry and dynamics of meandering rivers. Geol. Soc. Am. Bull. 110, 1485–1498.
Termini, D., Piraino, M., 2011. Experimental analysis of cross-sectional flow motion in a large amplitude meandering bend. Earth Surf. Process. Landf. 36, 244–256.
Thompson, D.M., 2003. A geomorphic explanation for a meander cutoff following channel relocation of a coarse-bedded river. Environ. Manag. 31, 385–400.
Timar, G., 2003. Controls on channel sinuosity changes: a case study of the Tisza River, the Great Hungarian Plain. Quat. Sci. Rev. 22, 2199–2207.
van Dijk, W.M., van de Lageweg, W.I., Kleinhans, M.G., 2012. Experimental meandering river with chute cutoffs. J. Geophys. Res. Earth Surf. 117.
Wang, Y.F., et al., 1995. Sedimentological evidence of piracy of fossil Zoige Lake by the Yellow River. Chin. Sci. Bull. 40, 1539–1544.
Wasklewicz, T.A., Anderson, S., Liu, P.S., 2004. Geomorphic context of channel locational probabilities along the Lower Mississippi River, USA. Geomorphology 63, 145–158.
Wellmeyer, J.L., Slattery, M.C., Phillips, J.D., 2005. Quantifying downstream impacts of impoundment on flow regime and channel planform, lower Trinity River, Texas. Geomorphology 69, 1–13.
Xiao, D.R., Tian, B., Tian, K., Yang, Y., 2010. Landscape patterns and their changes in Sichuan Ruoergai wetland national nature reserve. Acta Ecol. Sin. 30, 27–32.
Zavattero, E., Du, M.X., Ma, Q., Delestre, O., Gourbesville, P., 2016. 2D sediment transport modelling in high energy river-application to Var River, France. Procedia Eng. 154, 536–543.
Zinger, J.A., Rhoads, B.L., Best, J.L., 2011. Extreme sediment pulses generated by bend cutoffs along a large meandering river. Nat. Geosci. 4, 675–678.